Fullerenes

DOI: 10.1002/anie.200906023

Isolation of a Small Carbon Nanotube: The Surprising Appearance of $D_{5h}(1)$-C_{90}**

Hua Yang, Christine M. Beavers, Zhimin Wang, An Jiang, Ziyang Liu, Hongxiao Jin,* Brandon Q. Mercado, Marilyn M. Olmstead,* and Alan L. Balch**

Since the macroscopic synthesis of C_{60} and C_{70} in 1990,[1] the fullerene family has drawn attention with potential applications in a wide range of scientific and industrial areas. C_{60}, C_{70}, C_{76}, C_{78}, and C_{84} have become well-known; however, the carbon soot from arc generators contains small amounts (generally less than 1%) of higher fullerenes. The isolation of these higher fullerenes in isomerically pure form is challenging, especially since the number of isomers that follow the isolated-pentagon rule (IPR) increases as the size of the fullerene cage expands.[2] The isolated-pentagon rule requires that each pentagon be surrounded by five hexagons to avoid strain-inducing pentagon–pentagon contact.

There are 46 isomers of C_{90} that obey the IPR, but none of these has been obtained in pure form. In regard to unfunctionalized C_{90}, Achiba et al. utilized ^{13}C NMR spectroscopy to determine that an enriched sample of C_{90} contained five isomers: one with C_{2v} symmetry, three with C_2 symmetry, and one with C_1 symmetry.[3] Shi and co-workers reported the separation and UV/Vis spectra of two isomers of C_{90} from arc-generated carbon soot obtained from ytterbium-doped graphite rods.[4]

Several computational studies have been performed to better understand which specific isomers are expected to be stable.[5–8] Slanina et al. concluded from semiempirical quantum-chemical calculations that the $C_2(45)$, $C_{2v}(46)$, $C_s(35)$, $C_2(18)$, and $C_1(9)$ isomers are likely to be the most stable at the temperatures used for C_{90} production.[6] Computations at the B3LYP/6-31G level by Sun indicated that the $C_2(45)$ isomer was the most stable, and $C_2(28)$, $C_1(30)$, $C_1(32)$, $C_s(35)$, $C_2(40)$, and $C_{2v}(46)$ were other stable isomers.[7] Watanabe et al. performed PM3 computations and concluded that there are 11 isomers ($D_{5h}(1)$, $C_1(27)$, $C_2(28)$, $C_1(29)$, $C_1(30)$, $C_1(31)$, $C_1(32)$, $C_s(34)$, $C_s(35)$, $C_2(45)$, and $C_{2v}(46)$) that are kinetically as well as thermodynamically stable.[8]

Some adducts of C_{90} have also been structurally identified. Recently, a trifluoromethyl adduct of C_{90}, $C_{90}(CF_3)_{12}$, which was synthesized by the free-radical addition of CF_3I to a mixture of higher fullerenes, was shown through ^{19}F NMR spectroscopy to utilize the $C_1(32)$-C_{90} cage.[9] The chlorination of a mixture of higher fullerenes through treatment with $SbCl_5$ yielded a crystalline material containing $C_{90}Cl_{32}$.[10] Crystallographic analysis revealed that a single crystal contained a mixture of two isomers that utilized the $C_{2v}(46)$-C_{90} and $C_s(34)$-C_{90} cages.

Carbon soot was obtained by vaporizing a graphite rod filled with Sm_2O_3 and graphite powder in an electric arc as outlined previously.[11,12] The carbon soot was extracted with *o*-dichlorobenzene, and the soluble extract was subjected to a multistage high pressure liquid chromatographic (HPLC) isolation process involving three complementary chromatographic columns (Buckyprep-M, Buckyprep, and 5PBB) with either chlorobenzene or toluene as the eluent. Three individual isomers of C_{90} were identified and purified. These isomers are labeled C_{90}(I), C_{90}(II), and C_{90}(III) in the order of their chromatographic elution times. Figure 1 shows the HPLC chromatogram and laser desorption ionization time-of-flight (LDI-TOF) mass spectrum of the purified sample of the first-eluted isomer, C_{90}(I).

We obtained isomer-free C_{90}(II) and C_{90}(III) in a similar fashion (see the Supporting Information). C_{90}(I) differs distinctly from C_{90}(II) and C_{90}(III) in terms of its retention time (Table 1). The unusually short retention time observed for C_{90}(I) on the polar stationary phases of both the phenothiazine-derivatized Buckyprep-M and pentabromobenzyl (5PBB) columns suggested that it is less polar than C_{90}(II) or C_{90}(III), whereas the relatively long retention time on the nonpolar pyrenylethyl silica of the Buckyprep column suggested that C_{90}(I) has a more elongated structure that enables better π–π interaction with the stationary phase.[13]

The three isomers of C_{90} display quite different UV/Vis/near-infrared (NIR) absorption behavior (Figure 2). C_{90}(I) produces two characteristic absorptions at 484 and 589 nm, whereas C_{90}(II) exhibits a strong band with strong but poorly resolved peaks around 413 and 453 nm, and C_{90}(III) shows an almost featureless spectrum with broad bands at 602 and

[*] H. Yang, Z.-M. Wang, A. Jiang, Prof. Dr. Z.-Y. Liu
Department of Chemistry, Zhejiang University
Hangzhou 310027 (China)
Fax: (+86) 571-8795-1895
E-mail: zyliu@zju.edu.cn

B. Q. Mercado, Prof. Dr. M. M. Olmstead, Prof. Dr. A. L. Balch
Department of Chemistry, University of California
Davis, CA 95616 (USA)
E-mail: mmolmstead@ucdavis.edu
albalch@ucdavis.edu

Dr. C. M. Beavers
Advanced Light Source, Lawrence Berkeley National Laboratory
1 Cyclotron Road, Berkeley, CA 94720 (USA)

Dr. H.-X. Jin
College of Materials Science and Engineering
China Jiliang University, Hangzhou 310018 (China)

[**] Z.-Y.L. thanks the National Natural Science Foundation of China (20971108), and A.L.B and M.M.O. thank the National Science Foundation (CHE-0716843) for support. The Advanced Light Source is supported by the Director, Office of Science, Office of Basic Energy Sciences, U.S. DOE (Contract No. DE-AC02-05CH11231).

Supporting information for this article is available on the WWW under http://dx.doi.org/10.1002/anie.200906023.

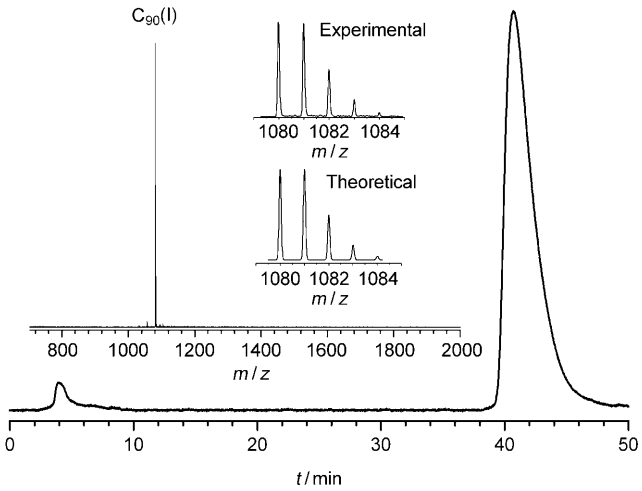

Figure 1. HPLC profile of C_{90}(I) on a Buckyprep column (10×250 mm^2) with toluene as the eluent (4.0 mL min^{-1}). The inset shows the LDI-TOF mass spectrum and expansions of the experimental and theoretical isotope distributions for C_{90}(I).

Table 1: Retention time of isomers of C_{90} (I, II, III) on three different HPLC columns.

Isomer	t_R [min]		
	Buckyprep-M[a]	Buckyprep[b]	5PBB[c]
C_{90}(I)	17.5	40.2	23.5
C_{90}(II)	21.6	38.3	30.0
C_{90}(III)	21.6	40.4	30.0

[a] Flow rate: 4.0 mL min^{-1}; eluent: toluene. [b] Flow rate: 4.5 mL min^{-1}; eluent: toluene. [c] Flow rate: 4.5 mL min^{-1}; eluent: chlorobenzene.

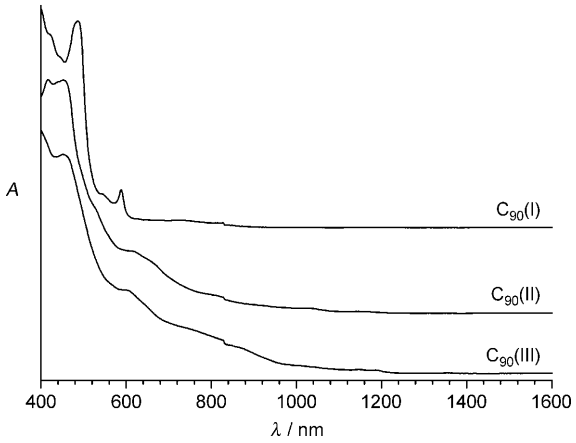

Figure 2. UV/Vis/NIR absorption spectra of the isolated C_{90} isomers dissolved in carbon disulfide.

452 nm. The absorption onsets of C_{90}(I), C_{90}(II), and C_{90}(III) were 920, 1230, and 1253 nm, which correspond to HOMO–LUMO band gaps of 1.34, 1.00, and 0.98 eV, respectively. These values are far smaller than that of C_{60} (1.90 eV),[14] but larger than those of the nine isomers of C_{84} isolated to date, with the exception of D_{2d}(I)-C_{84}.[13] These observations contradict the old assumption that the HOMO–LUMO gap decreases as the number of atoms in the fullerene increases. The UV/Vis spectrum reported herein for C_{90}(I) is different from the spectra reported by Shi and co-workers for their two C_{90} isomers.[4] Our C_{90}(II) and C_{90}(III) isomers have similar absorption peaks to those reported by Shi and co-workers for their isomers C_{90}(I) and C_{90}(II), respectively.

Black crystals of $[D_{5h}(1)$-$C_{90}\cdot Ni^{II}(oep)]$ (oep = 2,3,7,8,12,13,17,18-octaethylporphyrin dianion) were obtained by the slow diffusion of solutions of C_{90}(I) and $[Ni^{II}(oep)]$ in toluene. Diffraction data were collected at Beamline 11.3.1 at the Advanced Light Source with 0.7749 Å synchrotron radiation, and then solved and refined by standard procedures. The asymmetric unit consists of one fully ordered molecule of $D_{5h}(1)$-C_{90} and two half molecules of $[Ni^{II}(oep)]$ with the other halves generated by inversion.

Figure 3 shows the structure of the fullerene, which is a short armchair endcapped nanotube with D_{5h} symmetry. The

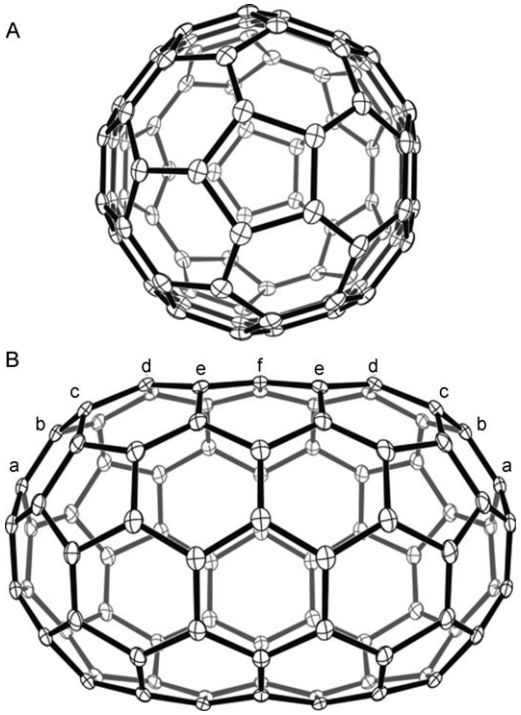

Figure 3. Two orthogonal views of C_{90}(I) ($D_{5h}(1)$-C_{90}) from crystalline $[D_{5h}(1)$-$C_{90}\cdot Ni^{II}(oep)]$ showing 30% thermal contours.

two poles have C_{60}-like structures. To form $D_{5h}(1)$-C_{90} from C_{60}, the latter is cut in half, one half is rotated by 36° relative to the other, and 30 carbon atoms are inserted in planar sets of ten. The carbon atoms in $D_{5h}(1)$-C_{90} are arranged in eleven layers. The unique layers are designated a–f in Figure 3. Thus, in idealized $D_{5h}(1)$-C_{90} there are six types of carbon atoms and ten types of C–C bonds (between carbon atoms a,a, a,b, b,c, c,c, c,d, d,d, d,e, e,e, e,f, and f,f). $D_{5h}(1)$-C_{90} is a member of a set of nanotube-like fullerenes with the formula C_{60+10n}, which have alternating D_{5h} (when n is odd) or D_{5d} symmetry (when n is even). The structure of $D_{5h}(1)$-C_{90} ($n=3$) is thus closely related to that of C_{70} ($n=1$).

To gain an understanding of the structure and stability of this novel nanotube, we performed DFT computations at the B3LYP/6-31G(d) level for $D_{5h}(1)$-C_{90}. Figure 4 shows the

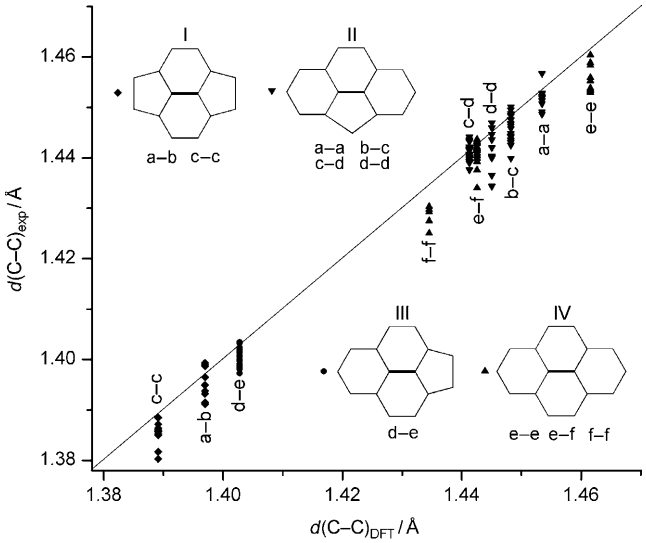

Figure 4. Correlation between the experimental and calculated C–C bond distances in D_{5h}-C_{90}. Distances are labeled by bond type and coded with respect to the structural fragment.

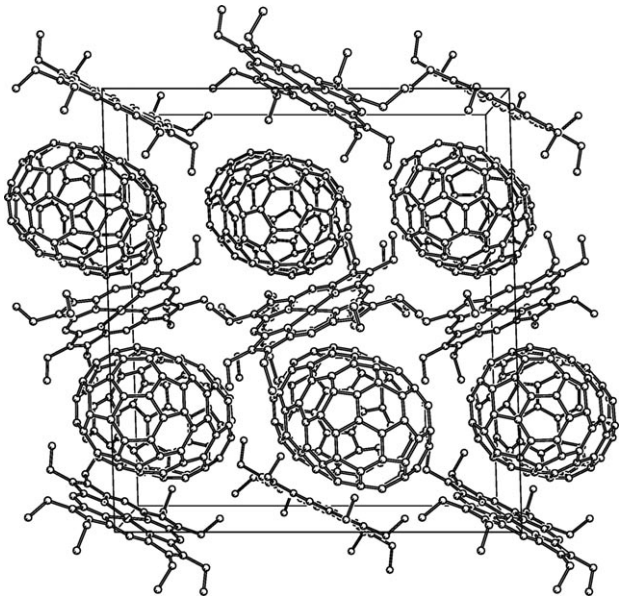

Figure 5. A perspective view of [C_{90}·Ni(oep)] with atoms denoted by uniform circles of arbitrary size.

correlation between the C–C bond lengths determined experimentally by X-ray crystallography on [D_{5h}(1)-C_{90}·Ni^{II}-(oep)] and those determined theoretically for the optimized structure. A good correlation is seen, although the computation seems to systematically overestimate the C–C bond lengths by a small amount. The experimental C–C bond lengths vary from 1.38 to 1.48 Å. The two shortest sets of C–C distances were found for the bonds between the c,c and a,b carbon atoms at the end caps of this small nanotube. These atoms are the central parts of the only pyracylene (type I) sites on the fullerene surface. The situation in C_{70} is similar; again, the shortest C–C distances are the bonds at the poles between the corresponding c,c and a,b carbon atoms.[15,16] To further compare D_{5h}(1)-C_{90} with C_{70}, we examined the pyramidalization (POAV) angles for the carbon atoms in these fullerenes.[17] For C_{60}, the POAV angle is 11.64(10).[17] For D_{5h}(1)-C_{90}, the POAV angles are: a, 11.91(8); b, 11.95(9); c, 11.70(15); d, 10.37(19); e, 7.2(2); f, 5.51(15)°; the corresponding angles for C_{70} are: a, 11.87(9); b, 12.01(9); c, 11.44 (16); d, 10.18(17); e, 8.66(16)°.[16] The POAV angles for the a-type carbon atoms in D_{5h}(1)-C_{90} and in C_{70} are slightly larger than that of C_{60}. As one moves from layer a to layer f in D_{5h}(1)-C_{90}, the POAV angles gradually decline.

In D_{5h}(1)-C_{90}, the hexagonal rings at the center of the molecule are not planar but are bent inward in a butterfly-like arrangement. The average dihedral angle for the hexagonal rings with a pair of f-type carbon atoms in *para* positions is 157.0(3)°, whereas for the hexagons with e-type carbon atoms in *para* positions, the degree of folding is less, and the corresponding dihedral angle is 162.6(2)°. The hexagons with two d-type carbon atoms in *para* positions are nearly planar with an average dihedral angle of 176.6(3)°.

Figure 5 shows the interrelationships between the fullerene and the porphyrin. Each cylindrical D_{5h}(1)-C_{90} cage is surrounded by two different [Ni(oep)] molecules in a clamshell arrangement. The dihedral angle between the planes of the two different [Ni(oep)] molecules is approximately 60°. The placement of the two [Ni(oep)] molecules about the D_{5h}(1)-C_{90} molecule is asymmetric. The shortest distance between the nickel ions and the fullerene carbon atoms is 2.9441(9) Å for Ni2 and 3.1230(10) Å for Ni1. Likewise, each [Ni(oep)] molecule is sandwiched between two D_{5h}(1)-C_{90} molecules. This arrangement lacks the close face-to-face porphyrin–porphyrin contact that is generally seen for cocrystals of [Ni(oep)] with fullerenes or endohedral fullerenes.[12,18,19] Rather than all eight ethyl groups of an [Ni(oep)] molecule embracing a single fullerene, as is common in other fullerene–porphyrin cocrystals, the ethyl groups in [D_{5h}(1)-C_{90}·Ni^{II}(oep)] are arranged so that they can embrace the fullerenes on either side. The arrangement of these ethyl groups differs in the two [Ni(oep)] molecules. In one, the ethyl groups are arranged in a four-up, four-down fashion, whereas in the other the pattern is two up, one down, one up, two down, one up, one down. Interestingly, there are other cases in which the ethyl groups adopt a four-up, four-down arrangement but manage to retain the face-to-face contact that is absent in [D_{5h}(1)-C_{90}·Ni^{II}(oep)].[18,20]

To provide insight into the nature of the interactions between the fullerene cage of D_{5h}(1)-C_{90} and the metalloporphyrin, we obtained individual electrostatic potential maps of D_{5h}(1)-C_{90} and [Ni^{II}(oep)] at the B3LYP/6-31G(d,p) level of density functional theory (Figure 6).[8] The central belt of hexagons in D_{5h}(1)-C_{90} shows a region of significant positive potential as indicated by the deep-blue coloration (Figure 6b). In contrast, the central N_4 region of [Ni^{II}(oep)] is an area of negative potential, as denoted by the red coloration (Figure 6a). Thus, these two portions of the fullerene and the metal porphyrin have complementary regions of surface charge. The locations of these complementary regions account for the positioning of the two molecules relative to one another.

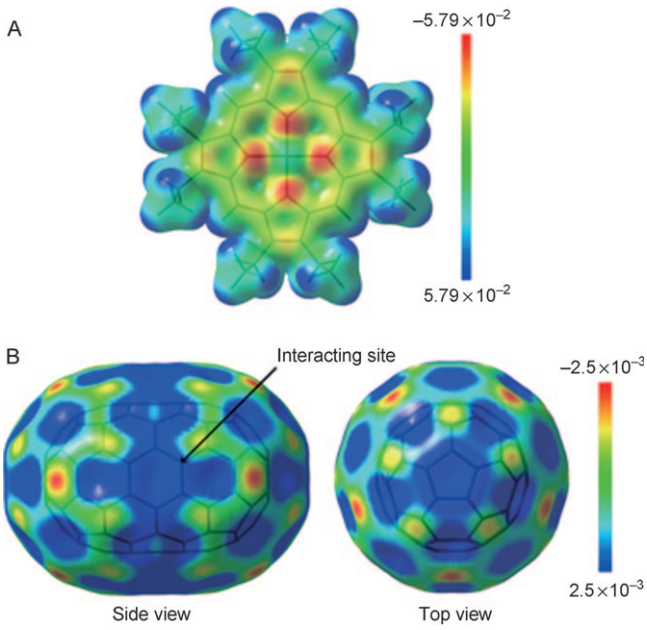

Figure 6. Molecular electrostatic potential mapping on the isosurface of the total electron density of A) [Ni^{II}(oep)] (0.01 e bohr^{-3}) and B) D_{5h}(I)-C_{90} (0.001 e bohr^{-3}).

The discovery of D_{5h}(1)-C_{90} as the major C_{90} isomer in our preparations is surprising. The ^{13}C NMR spectroscopic studies of Achiba et al.[3] produced no evidence for the presence of D_{5h}(1)-C_{90} in their samples, and the products obtained upon functionalization did not reveal the presence of the D_{5h} isomer either.[9,10] It has been reported that the incorporation of metal salts in the graphite rods used in the electric-arc synthesis can change the composition of fullerenes formed. For example, the addition of gadolinium to the graphite electrodes led to the isolation of isomers D_{3d}-C_{84} and D_{6h}-C_{84}.[21] The introduction of copper(II) nitrate into the graphite rods lowers the yields of empty-cage fullerenes relative to endohedral fullerenes in the electric-arc procedure.[22] The addition of metal salts of cerium, lanthanum, or yttrium to the graphite electrodes resulted in altered amounts of the higher fullerenes.[9] Thus, in our study, the presence of Sm_2O_3 during arcing appears to be responsible for directing the synthesis toward the formation of relatively large amounts of D_{5h}(1)-C_{90}.

The identification of D_{5h}(1)-C_{90} as the major C_{90} isomer produced by arcing of Sm_2O_3-doped graphite rods has implications regarding the mechanism of fullerene-cage formation. Many fullerene cages can be converted into another isomer through the Stone–Wales transformation (Scheme 1), and it has been suggested that the isomers of various fullerene cages are annealed through Stone–Wales transformation to produce the array of stable isomers that can be isolated.[2,23] The map of possible Stone–Wales transformations for C_{90} isomers shows that almost all isomers form a large, interconnected domain, but that D_{5h}(1)-C_{90} stands alone, and is not connected to any other isomer by the Stone-Wales transformation.[23]

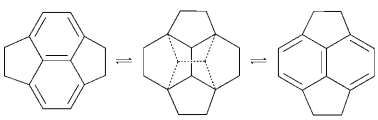

Scheme 1. The Stone–Wales transformation.

In summary, three pure isomers of C_{90} have been isolated from the raw soot produced from Sm_2O_3-doped graphite rods. Under these conditions, D_{5h}(1)-C_{90} is the major isomer of C_{90} produced. The products were isolated and separated by multistage HPLC and characterized by mass spectroscopy and UV/Vis/NIR measurements. The structure of the most abundant isomer was determined by single-crystal X-ray diffraction to be distinctly nanotube-like. Recently, we reported the isolation and structural characterization of a related nanocapsule, $Sm_2@D_{3d}$(822)-C_{104}.[24]

Experimental Section

Crystal data for [D_{5h}(1)-C_{90}·Ni^{II}(oep)]: black parallelepiped, 0.24 × 0.22 × 0.18 mm^3, monoclinic, space group $P2_1/c$, a = 24.2111(12), b = 13.1462(6), c = 22.1772(11) Å, β = 91.630(3)°, V = 7055.8(6) Å^3, λ = 0.77490 Å, Z = 4, ρ_{calcd} = 1.574 Mg m^{-3}; μ = 0.432 mm^{-1}; T = 100(2) K; ALS Beamline 11.3.1 Bruker Apex2 CCD detector; ω scans, $2\Theta_{max}$ = 80; 340704 reflections collected, 33420 independent (R_{int} = 0.0500) included in the refinement; min/max transmission = 0.90/0.93 (TWINABS-2008/2);[25] direct-methods solution (SHELXS97);[26] full-matrix least squares based on F^2 (SHELXL97);[26] R = 0.0438, wR = 0.1101 for all data; conventional $R1$ = 0.0397 computed for 30630 observed data ($I > 2\sigma(I)$) with 1192 parameters and no restraints.

CCDC 752363 contains the supplementary crystallographic data for this paper. These data can be obtained free of charge from The Cambridge Crystallographic Data Centre via www.ccdc.cam.ac.uk/data_request/cif.

Received: October 26, 2009
Published online: December 18, 2009

Keywords: carbon nanotubes · fullerenes · samarium · X-ray diffraction

[1] W. Krätschmer, L. D. Lamb, K. Fostiropoulos, D. R. Huffman, *Nature* **1990**, *347*, 354–358.
[2] P. W. Fowler, D. E. Manolopoulos, *An Atlas of Fullerenes*, Clarendon, Oxford, **1995**.
[3] a) Y. Achiba, K. Kikuchi, Y. Aihara, T. Wakabayashi, Y. Miyake, M. Kainosho, *Mater. Res. Soc. Symp. Proc.* **1995**, *359*, 3–9; b) Y. Achiba, K. Kikuchi, Y. Aihara, T. Wakabayashi, Y. Miyake, M. Kainosho in *The Chemical Physics of Fullerenes 10 (and 5) Years Later* (Ed.: W. Andreoni), Kluwer, Dordrecht, **1996**, pp. 139–147.
[4] J. Xu, Z. Wang, Z. Shi, Z. Gu, *Chem. Phys. Lett.* **2005**, *409*, 192–196.
[5] S. Okada, S. Saito, *Chem. Phys. Lett.* **1995**, *247*, 69–78.
[6] Z. Slanina, X. Zhao, S.-L. Lee, E. Osawa, *Chem. Phys.* **1997**, *219*, 193–200.
[7] G. Sun, *Chem. Phys.* **2003**, *289*, 371–380.
[8] M. Watanabe, D. Ishimaru, N. Mizorogi, M. Kiuchi, J. Aihara, *J. Mol. Struct. THEOCHEM* **2005**, *726*, 11–16.
[9] I. E. Kareev, A. A. Popov, I. V. Kuvychko, N. B. Shustova, S. F. Lebedkin, V. P. Bubnov, O. P. Anderson, K. Seppelt, S. H. Strauss, O. V. Boltalina, *J. Am. Chem. Soc.* **2008**, *130*, 13471–13489.

[10] E. Kemnitz, S. I. Troyanov, *Angew. Chem.* **2009**, *121*, 2622 – 2625; *Angew. Chem. Int. Ed.* **2009**, *48*, 2584 – 2587.
[11] D.-Y. Sun, Z.-Y. Liu, X.-H. Guo, W.-G. Xu, S.-Y. Liu, *J. Phys. Chem. B* **1997**, *101*, 3927 – 3930.
[12] H. Yang, C. Lu, Z. Liu, H. Jin, Y. Che, M. M. Olmstead, A. L. Balch, *J. Am. Chem. Soc.* **2008**, *130*, 17296 – 17300.
[13] a) T. J. S. Dennis, T. Kai, K. Asato, T. Tomiyama, H. Shinohara, T. Yoshida, Y. Kobayashi, H. Ishiwatari, Y. Miyake, K. Kikuchi, Y. Achiba, *J. Phys. Chem. A* **1999**, *103*, 8747 – 8752; b) C. R. Wang, T. Sugai, T. Kai, T. Tomiyama, H. Shinohara, *Chem. Commun.* **2000**, 557 – 558.
[14] J. H. Weaver, J. L. Martins, T. Komeda, Y. Chen, T. R. Ohno, G. H. Kroll, N. Troullier, R. E. Haufler, R. E. Smalley, *Phys. Rev. Lett.* **1991**, *66*, 1741 – 1744.
[15] A. L. Balch, V. J. Catalano, J. W. Lee, M. M. Olmstead, S. R. Parkin, *J. Am. Chem. Soc.* **1991**, *113*, 8953 – 8955.
[16] D. Pham, J. Ceron-Bertran, M. M. Olmstead, M. Mascal, A. L. Balch, *Cryst. Growth Des.* **2007**, *7*, 75 – 82.
[17] R. C. Haddon, K. Raghavachari, *Buckminsterfullerenes*, VCH, New York, **1993**, chap. 7.
[18] M. M. Olmstead, A. de Bettencourt-Dias, H. M. Lee, D. Pham, A. L. Balch, *Dalton Trans.* **2003**, 3227 – 3232.
[19] M. M. Olmstead, D. A. Costa, K. Maitra, B. C. Noll, S. L. Phillips, P. M. Van Calcar, A. L. Balch, *J. Am. Chem. Soc.* **1999**, *121*, 7090 – 7097.
[20] H. M. Lee, M. M. Olmstead, T. Suetsuna, H. Shimotani, N. Dragoe, R. J. Cross, K. Kitazawa, A. L. Balch, *Chem. Commun.* **2002**, 1352 – 1353.
[21] N. Tagmatarchis, A. G. Avent, K. Prassides, T. J. S. Dennis, H. Shinohara, *Chem. Commun.* **1999**, 1023 – 1024.
[22] S. Stevenson, M. C. Thompson, H. L. Coumbe, M. A. Mackey, C. E. Coumbe, J. P. Phillips, *J. Am. Chem. Soc.* **2007**, *129*, 16257 – 16262.
[23] E. Osawa, H. Ueno, M. Yoshida, Z. Slanina, X. Zhao, M. Nishiyama, H. Saito, *J. Chem. Soc. Perkin Trans. 2* **1998**, 943 – 950.
[24] B. Q. Mercado, A. Jiang, H. Yang, Z. Wang, H. Jin, Z. Liu, M. M. Olmstead, A. L. Balch, *Angew. Chem.* **2009**, *121*, 9278 – 9280; *Angew. Chem. Int. Ed.* **2009**, *48*, 9114 – 9116.
[25] G. M. Sheldrick, TWINABS, University of Göttingen, Germany, **1996**.
[26] G. M. Sheldrick, *Acta Crystallogr. Sect. A* **2008**, *64*, 112 – 122.

